Original Research Paper

Analysis of the Operation of DC Interconnected Households PV under Weather Conditions

[1,2]**Gilbert Ngoma** (iD), [1,3]**Maryse Dadina Nkoua Ngavouka** (iD), [4]**Azeddine Houari**, [5]**Léonide Messo** and [1,3]**Bernard M'Passi-Mabiala** (iD)

[1]*Department of Physics, Faculty of Science and Technology, Marien Ngouabi University, Brazzaville, BP 69, Congo*
[2]*National Institute for Research in Engineering Sciences, Innovation and Technology, (INRSIIT), Brazzaville, Congo*
[3]*Nanomaterials and Nanotechnologies Research Unit, National Research Institute in Exact and Natural Sciences (IRSEN), Brazzaville, Congo*
[4]*Nantes Atlantique Electrical Energy Research Institute, University of Nante, Saint-Nazaire, France*
[5]*Ecole Nationale Supérieure Polytechnique (ENSP), Marien Ngouabi University, Brazzaville, BP 69, Congo*

Abstract: Installing Photovoltaic (PV) systems is becoming a viable solution for rural areas, with an innovative approach consisting of interconnecting autonomous PV-powered households. This study analyses the performance of interconnected autonomous PV households under different weather conditions using the Matlab Simulink R2016a software. Over and above this interconnection analysis, in this study, a new mathematical model to predict PV power is also proposed and compared to the simulation's results and other approaches allowing to prosumer to control their interconnection to others. The interconnection demonstrated the improving performance of microgrids and mutual energy compensation, increasing efficiency by 9% in houses with a deficit. To manage the energy flow of these autonomous houses, the households' energy management is independent and the bus Voltage (Vdc) is maintained at around 52V, corresponding to the maximum bus voltage setpoint, thanks to integrated Proportional control (PI). The results of the simulation of the interconnection using the Matlab Simulink R2016a software show that irradiation and temperature have an impact on photovoltaic production and the results of the new mathematical approach are approximately 2% of those of the simulations.

Keywords: Stand-Alone Photovoltaic System, Battery Storage, Micro Grid, PV Power Prediction, Energy Management, P2P

Introduction

The move towards renewable energy is a response to growing environmental concerns and the limited supply of non-renewable resources (Schwarz *et al*., 2023). In addition, many communities in general and in the Republic of Congo in particular do not have adequate access to electricity. The Republic of Congo, in terms of electricity production in 2018, had 0.6 GW of installed generation capacity, mainly composed of hydroelectricity (0.2 GW) and fossil fuels (0.4 GW). Most of the growth in electricity capacity comes from the natural gas central. The installed hydroelectric capacity comes from three existing hydropower plants: Imboulou (120 MW), Moukoukoulou (74 MW) and Djouè (15 MW) according to the Energy Ministry. The Republic of the Congo is highly reliant on natural gas and the total of Renewable Energy (RE) installed is under 40% of the total capacity). In fact, the country has significant untapped renewable energy capacity, for example in solar energy the average irradiance is 4.5 kWh/m^2/day, compared with just 3 kWh/m^2/day in the temperate zone of Europe, which constitutes good potential for solar energy production according to Energy Ministry of Congo.

It is obvious that the world has high solar irradiance and many studies are being conducted in this domain as mentioned (Ngonda *et al*., 2023).

In that way, a study was carried out into the solar energy resources and Photovoltaic (PV) energy potential in the case of an under-utilized region in South Africa. They reported that Alice has abundant solar resources for the use of solar Panels (PV) and are comparable to other regions of the world. In South Africa, the town experiences a total annual global horizontal irradiance of

approximately 4.98 kWh/m^2 per day, according to the GSA (Overen and Meyer, 2022).

In Southern Algeria, a study on the analytical evaluation of the hot, dry climate, outdoor performance and efficiency of grid-connected PV systems (Necaibia *et al*., 2018) revealed an average of 4.88 kWh/kWp/day per year and a solar energy performance rate of 74%. In Slovenia, a study adopted similar parameters to assess the performance of 3326 solar PV systems (Seme *et al*., 2019). The study showed that the final yield and capacity utilization factor was 1,038 kWh/kWp and 11.85%, while the performance rate was 68.84%. That is why, the Republic of Congo, which has an average annual solar radiation of around 1,700 kWh/m^2, or 4.7 kWh/m^2.d according to data from the Agence Nationale de l'Aviation Civile (ANAC), has just started to promote renewable energies in response to the high cost of using oil and the transport of energy to isolated areas. One of the renewable energies being promoted is PV. Unfortunately, this type of energy is intermittent and requires precise dimensioning. Thus, PV power plants require a large energy storage system to regulate voltage and reduce the effects of intermittency of the energy source, which increases the cost of the installation. Thus, several energy sources have been proposed to reduce the cost of Renewable Energy Storage (RES) in order to form an interconnected electricity grid (Vadirajacharya and Katti, 2012).

Beyond intermittency, the individual management of PV energy during the day for a stand-alone system is often another problem which is why, the microgrid and the storage are used.

In fact, The interconnection of stand-alone photovoltaic households with and without central storage, is indeed worthy of study, as it aligns with the growing importance of decentralized renewable energy systems, improving energy efficiency and reliability, promoting energy self-sufficiency, advancing control and optimization strategies.

In the literature, both the AC Micro Grid (ACMG) and the DC Micro Grid (DCMG) have been investigated. The study showed that the DCMG has certain advantages over the ACMG, such as ease of connection to the DC bus and system reliability, as well as high efficiency. They confirmed that in DCMGs, power disturbances are caused by fluctuating power exchanges, power variations between the storage system and energy sources, as well as rapid load change of the DC bus (Lonkar and Ponnaluri, 2015).

With this in mind, the study conducted by Ahshan *et al.* (2010), has designed an MG system that has the advantage of using renewable energy sources and reducing transmission losses when using wind and hydroelectric power.

The study by Phurailatpam *et al*. (2015) proposed a DCMG system that includes a PV power system and uses the battery as an energy storage system and the DC/DC

converters were also investigated, as well as Maximum Power Point Tracking (MPPT) for the PV system. The performance of their system at constant and varying values of the irradiance, wind speed and load was monitored and analyzed. The simulation results of that study showed that the system maintained the DC bus Voltage (Vdc) at a constant value, confirming the advantages of the DCMG over the ACMG.

Beyond PV system operation, power management is crucial, leading some authors to propose a new binary-based power management strategy (BPSO) to optimize MG performance, maximize MG power and reduce system power consumption (Elsied *et al*., 2016). A study by Mwinyiwiwa (2013) proposed limiting storage capacity by connecting multiple Distributed Renewable Energy sources (DERs) to the grid via a SEPIC converter. This method eliminates SEPIC converter voltage variations and staggered load variations. However, the number of DERs connected requires the AI controllers to meet conflicting requirements, which limits communication. The central Micro Grid Controller (MGCC) can be installed either on the low-voltage side or in the low-voltage substation (Lopes *et al*., 2006).

Implementing a Battery Energy Storage System (BESS) in DCMG improves its operation, thereby reducing its operating costs (Gil-González *et al*., 2020). Therefore, they proposed efficient operation strategies that maximize the useful life of BESS without making it operate inadequately or become completely discharged. In their study, they observed that this strategy also affects the performance of the DCMG and concluded that future work could include the development of operational strategies for BESS to minimize the DCMG's operating costs and increase its useful life.

Regarding the bus voltage, in the literature, the regulation voltage on the DC bus of an MG has been achieved (Madaci *et al*., 2016; Sahu *et al*., 2018). However, its stability remains a challenge, leading to voltage drops and rises when the voltage of inputs and outputs (loads connected to the DC bus) changes suddenly, regardless of their size. Contrary to the work of (Kumar *et al*., 2020), which considered constant input parameters and a variable load to evaluate the controller's performance.

It has been concluded in the literature that the shortcomings identified in the planning, operation and control of DC MG can be overcome through advanced technologies and further research (Al-Ismail, 2021).

Among recent technologies, in areas where solar potential is dominant, Peer-to-Peer (P2P) technology is being adopted (Zhang *et al*., 2018; Sayed *et al*., 2024; Kong *et al*., 2024; Harish *et al*., 2019; Choobineh *et al*., 2023). However, a lot of discussions have been going on peer-to-peer electricity sharing and trading in an MG scenario all over the world. With the advent of smart grids and transactive energy systems, the design of a reliable

electricity exchange model that can integrate the on-site generation of renewable energy sources, variable loads and households without rooftop solar PVs in an MG scenario, is necessary. All around the world, off-grid solar-based systems are being utilized to satisfy the electricity demands of isolated rural areas.

It is noticed in Congo as in many countries, in rural areas, everyone buys their own PV kit and installs it, while the other household overproduces energy when the load is insufficient, or underproduces when the load is too high (Hoffmann and Ansari, 2019). This overproduction in areas close to the national grid is injected into the national grid and, if necessary, withdrawn from it. This overproduction (Salles-Mardones *et al.*, 2022) is used to save energy consumption in residential houses with electric Vehicles in Chile.

In the same option, India has achieved good progress in managing the energy demand with a 0.5% energy deficit and in managing the peak demand with a 0.6% deficit in July 2019 (Central Electricity Authority, 2017) via the technology of P2P. The challenge, however, remains in delivering affordable power to all and reliability of service for rural electrification (Niti, 2017).

In a recent study, (Sayed *et al.*, 2024) investigated the feasibility of a Peer-to-Peer (P2P) solar energy-sharing system for rural communities. The results of the analysis show that the P2P system increased the community's self-sufficiency and self-consumption by 13.66 and 11.16%, respectively. As a result, a significant improvement in the life cycle enables the community to utilize the benefits of the proposed energy-sharing system.

In this type of sharing, (Kumar *et al.*, 2020) considered constant input parameters and variable load to evaluate the controller performance. Furthermore, in this study, the DC MG will be analyzed under different meteorological conditions with a point load and the input parameters, particularly irradiance and temperature, are variable.

The study by Harish *et al.* (2019) calculated surplus power at every hour sample of the simulation period, as the difference of on-site solar PV generation minus the hourly demand. However, no forecasting technique has been used here. The developed algorithm prioritizes satisfying the individual household's demand for the hour and any surplus available is for charging of battery or for P2P power sharing. Therefore, in this study, in order to control its connection to the grid without using simulation results, the power prediction is proposed using two meteorological parameters given by the meteorological prevision of the country. This mathematical approach enables autonomous households to predict daily production according to their needs and to decide whether or not to connect to the grid. Also, in the literature, the impact of meteorological conditions is not discussed in the P2P solar energy sharing system.

Hence, the scientific aim of this study is to analyze the operation of DC interconnected households under meteorological conditions in order to see the robustness of interconnection households in sharing energy. The integration of MG in these localities would be a reliable solution, as it would have a very positive socio-economic impact on the development of rural areas. It will provide electricity on a permanent basis, enabling the population to carry out certain activities at night. The study will focus on the interconnection of stand-alone households powered by PV systems with specific storage capacity, common load and central storage for household surpluses with a mathematical approach to predict the PV power at an hour of the day.

The novelty in this article is the contribution of the mathematical approach which allows users to program their interconnection control device (switch) for dispatching according to household needs. This approach will enable us to determine the interconnection conditions on the basis of meteorological data. In this article, we will also want to show the impact of sudden changes in irradiation on the load of a household and the behavior of interconnected households when they do not receive the same irradiation and temperature.

The objectives of this study are to:

– Study the behavior of DC MG voltage and power following weather conditions
– Propose a PV power prediction equation approach
– Evaluate the performance of the DC MG energy dispatching system

Theory and Calculation

Household Sizing

The energy balance consists of determining the daily energy consumption of all the electrical equipment in order to correctly size the system. The energy balance of a household is determined in Table (1) from which the daily energy of the MG is deduced.

The peak power Pc of the array is determined by taking into account the daily energy.

Table 1: Energy balance

Consumption	Power (W)	Quantity	Duration (h)	Energy (Wh/d)
lamps	10	5	5	250
TV	60	1	4.5	270
Radio	30	1	6	180
Others	360		1	360
Total daily energy				1 060

E and the average incident energy per day Gi:

$$Pc = \frac{E}{ki * Gi} \quad (1)$$

Where, ki is the correction coefficient for systems with battery banks, generally between 0.55 and 0.75. The approximate value used for systems with batteries is often 0.65 in areas where the minimum daily sunshine Gi is 2.5 kWh/d. In this study, ki is 0.38. The peak power corresponding to this study is around 600 Wp.

The capacity C of the battery is determined by the formula below:

$$C = \frac{E * N}{D * U} \quad (2)$$

With: C: Battery capacity in ampere-hours (Ah), E: Daily energy, N: Number of days of autonomy, D: maximum allowable discharge (for lead batteries, $D = 0.8$), U: Battery voltage (V).

Presentation of the System

The installation of photovoltaics in rural areas becomes a recommended option for the population, but its management often poses problems with variations in weather conditions. Thus, in this article, a model of autonomous PV MG is proposed (Figs.1-2) with a central storage system that can be used for a public establishment load.

In the practical context, comparing a line resistance of 0.01 Ohm, for a section of 10 mm^2, the distance between households is approximately 6 m for a copper resistivity of 0.018 μm. For the simulation, we use a computer branded ''hp Intel(R) Core(TM) i7-4510U CPU @ 2.00GHz 2.60 GHz and 16 GB RAM''.

Modeling of the DC-DC Boost Converter (Bidirectional)

In most PV installations, DC/DC converters or choppers are used for protection purposes, to manage battery overcharge or deep discharge problems, to optimize PV module operation and to manage output voltage fluctuations (Sun *et al.*, 2019). In the literature, there are three main types of choppers, depending on the role they play (Tan *et al.*, 2013; Zaouche *et al.*, 2017), in particular:

- The Boost chopper or booster: It raises the voltage level
- Buck or step-down: It lowers the voltage level
- The mixed buck-boost chopper

These converters are all made up of reactive elements (inductors, capacitors) which, in the ideal case, do not consume any energy. For the purpose of this study, the bidirectional boost converter used was developed in the literature by El-Shahat and Sumaiya (2019) and its electrical model is given by the following scheme (Fig. 3).
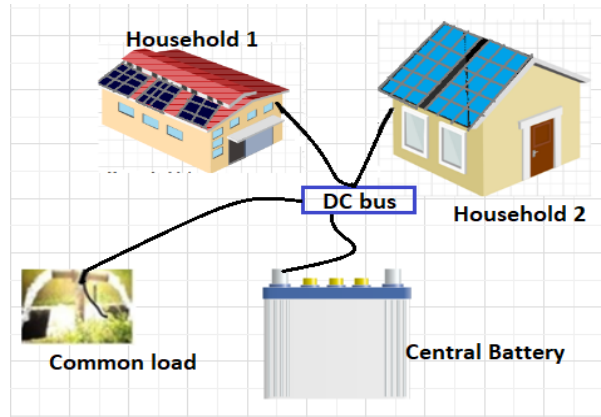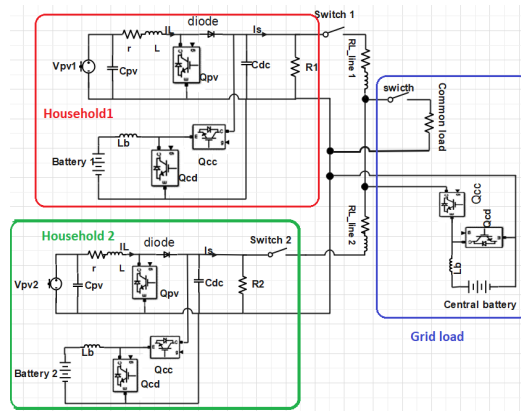

Fig. 1: Microgrid model

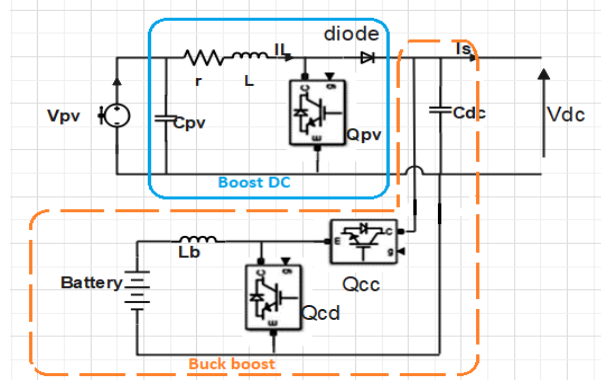**Fig. 2:** Electrical model of micro-grid

Fig. 3: DC-micro grid system circuit for stability analysis

Two controls are considered in the model. The control signals are the duty cycles of the converters. Qpv controls the power output of the PV; Qcc controls the DC bus voltage with Qcd equal to 1-Qcc.

The battery model used in this study is the electrical equivalent circuit in Matlab Simulink R2016a and its parameters are presented in Table (2) and the parameters of the PV module used are presented in Table (3).

Energy Management

Hybrid systems in general have some form of control. Control is sometimes individually integrated into each component of the system from the design stage (Li and Ho, 2021). Another command is the monitoring of all components. Some specific functions include starting and stopping to control the diesel generators, adjusting their operating points, battery charging and distributing power for different loads.

The Proportional, Integral (PI) regulator which is the corrector, is a system that allows to control and improvement of slavery performance (Nejat, 2022). Thanks to these high-performance qualities, it has been chosen to regulate the voltage of the system which will be maintained at around 52 V when the State of Charge (SoC) is around 100%. This value can be down to 42V which corresponds to 80% of the deep discharge of the batteries. The PI used is described in the Fig. (4).

Table 2: Battery parameters

Parameters	Values
Nominal voltage (V)	48
Rated capacity (Ah)	400
Initial state-of-charge (%)	100
Discharge	
Maximum capacity (Ah)	416
Cut-off Voltage (V)	42
Fully charged voltage (V)	52.26
Nominal discharge current (A)	80

Table 3: Parameters of the module type UNISON 150.12M

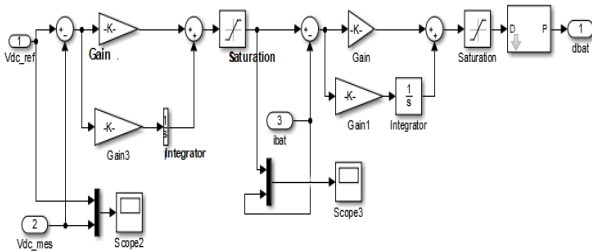| Description	Values
Power max (Pm)	150 W
Tolerance of power	0/+3%
Voltage with power max (Vmp)	17.8 V
No-load voltage (Voc)	21.3 V
Temperature coefficient—Pm	–0.43%/°C
Intensity with power max (Imp)	8.43 A
Intensity in short circuit (Icc/Isc)	9.1 A
NOCT/TUC **	45±2°C
Effectiveness of the modules	16.58%
Dimension of the module	1340×675×35 mm

Fig. 4: PI command simulated in Simulink

In this system, the energy management is done in such a way that, the producer is not deprived of his production, management is therefore individual (Querini *et al*., 2020; Nikmehr *et al*., 2017). Management is done according to time and power delivered. Thus, the energy produced by one of the houses is intended to first satisfy its own load.

On the other hand, when there is an energy deficit in a household, that is to say, the PV cannot satisfy the load (Ppv < Pch), then it will extract energy from the grid: It means, the energy coming from other households if not, from central storage. The common load, which could be solar pumping, receives the energy that is available on the grid. The central battery can only be charged if there is surplus production at the household level. In this energy management, when there is a fault in one of the households, this will not have an impact on other households. The algorithm used is simple and is presented in Fig. (5).

To see how effective, the energy dispatching is, each household controls its connection to the grid using a microcontroller switch (Fig. 6). For the management strategy, the following conditions have been set for each household:

- 1st household control: From 0-2.5s, no dispatching unless the PV power is >506 W; after 2.5s, household 1 is permanently connected to the grid
- 2nd household command: From 0-5 s, no dispatching unless PV power >60 W; after 3.5 s, household 2 is permanently connected to the grid.

These commands are applied up to the times shown here to validate the control algorithm using a control switch. After this time, the behavior of the grid in synchronization is observed.

To evaluate the effectiveness of the control strategy, the following conditions were examined according to the algorithm (Fig. 5):

- A: Ppv > P_{load}: The household load is powered by its PV and its PV recharges its battery with this surplus if the switch is on, it exchanges with the grid
- B: Ppv < P_{load}: The household load is powered both by its PV, its battery and by the power it draws from the grid if the switch is on
- C: Ppv <0: The household load is powered only by its battery when the household is not interconnected
- D: Ppv <0: The household load is powered by its battery and by the power drawn from the grid when there is interconnection

The Table (4) gives the parameters of households. The diagram simulated in Matlab Simulink R2016a for the system comprising battery, boost converter and PV is shown in Fig. (7).

Table 4: Parameters of households

Parameters	Values	Parameters	Values
Field 1 P_{PV}	600 Wp	Field 2 P_{PV}	600 Wp
I_{sc}	18.2 A	I_{sc}	18.2 A
V_{oc}	42.6 V	V_{oc}	42.6 V
V_{max}	35.6 V	V_{max}	35.6 V
I_{max}	16.86 A	I_{max}	16.86 A
Boost of Household 1		Boost of Household 2	
$R_{filtrepv}$	0.05 Ohms	$R_{filtrepv}$	0.05 Ohms
$L_{filtrepv}$	1e-1 H	$L_{filtrepv}$	1e-1 H
f_s	10 kHz	f_s	10 kHz
C_{pv}	100e-6 F	C_{pv}	100e-6 F
α	0.2	α	0.2
$Rline$	0.01 Ohm	$Rline$	0.01 Ohm
$Lline$	1e-3 H	$Lline$	1 H
	Battery 1		Battery 2
$R_{filtrebat}$	0.05 Ohm	$R_{filtrebat}$	0.05 Ohm
$L_{filtrebat}$	3e-3 H	$L_{filtrebat}$	3e-3 H
C_{dc}	3000e-6 F	C_{dc}	100e-6 F
$Vbat1$	48 V	$Vbat2$	48 V
Capacity	400 Ah	Capacity	400 Ah
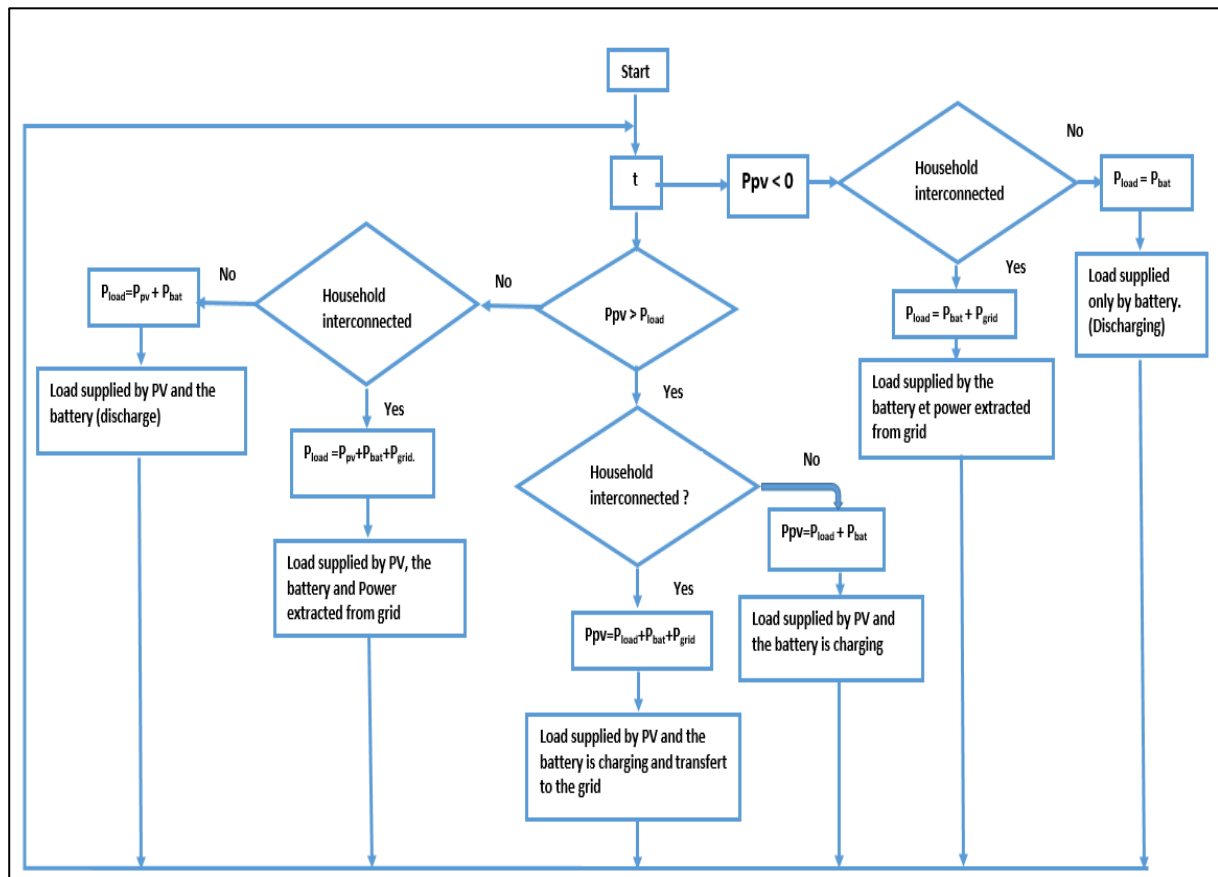
Fig. 5: Management algorithm
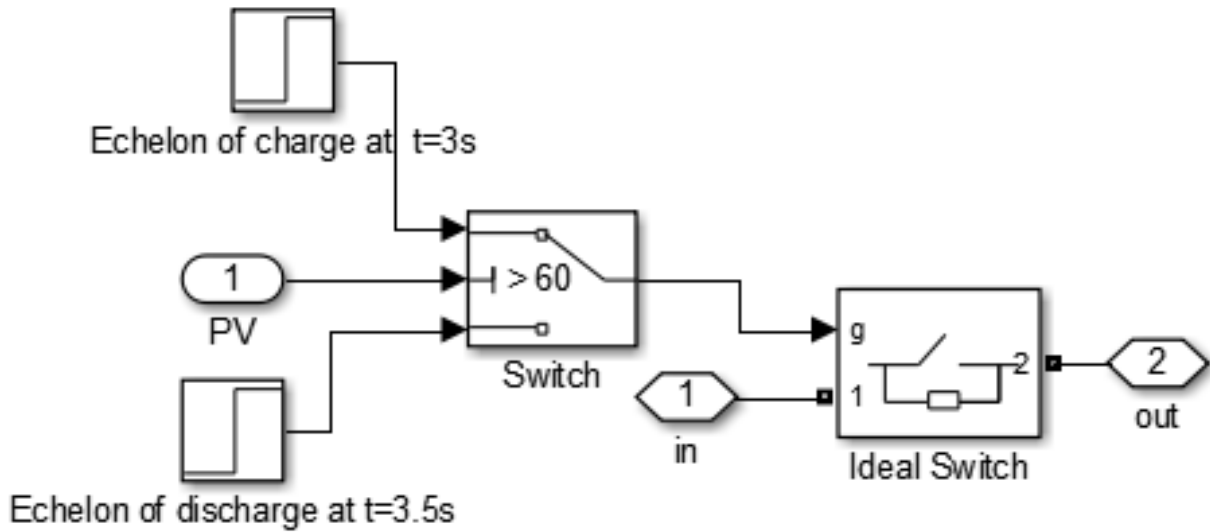
Fig. 6: The interconnect source control process
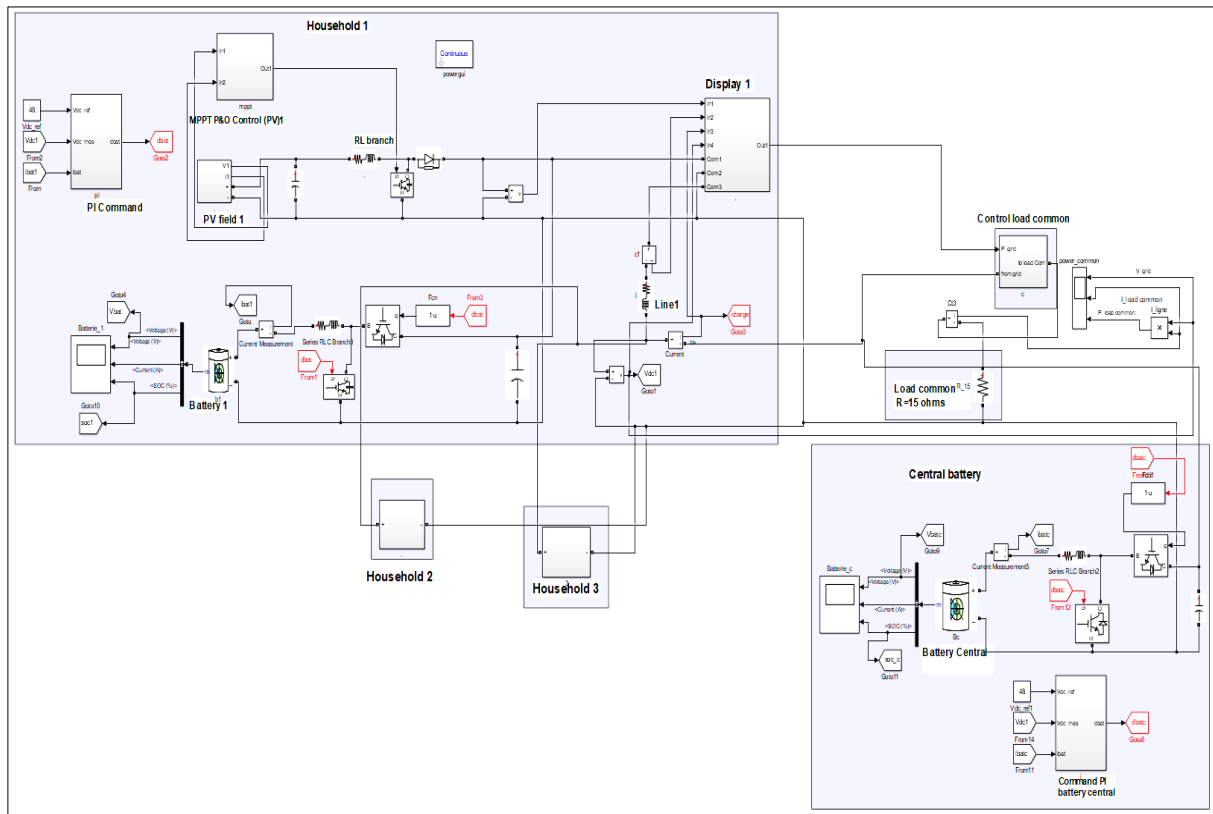
Fig. 7: Scheme of the microgrid with PI command in Matlab Simulink R2016a

Table 5: Parameters of the transistor used

Parameters	Values
Internal resistance Ron	1e-3 (Ohms)
Snubber resistance Rs	1e5 (Ohms)
Snubber capacitance Cs	Inf (F)

Theoretical Evaluation

In this part, two different households (different loads and irradiation) are presented.

The profiles of irradiance and temperature for households are presented.

17
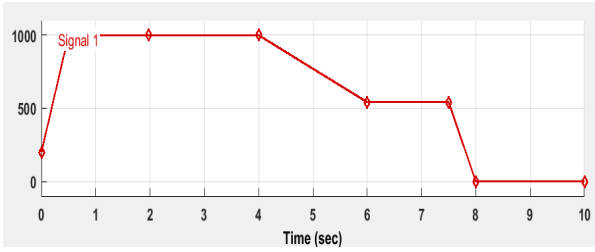
Fig. 8: Profile of irradiance 1
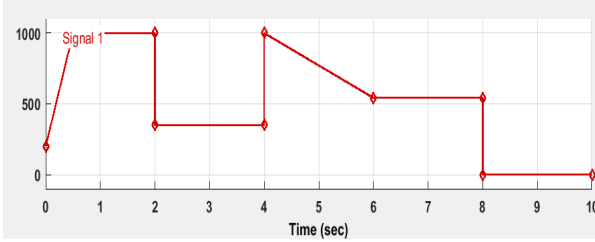
Fig. 9: Profile of irradiance 2
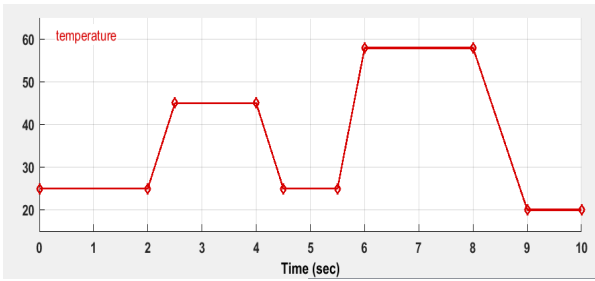
Fig. 10: Profile of temperature

The literature proposes several formulas to predict the theoretical power of modules as a function of weather conditions. For (Jie *et al*., 2007), this power is:

$$P_{thpv,j} = G * S * \eta * (1 - 0.0045 * (T - 25)) \tag{3}$$

η is the PV efficiency, T is the temperature measured on the panel (°C), S is the area of the solar panels (m^2) and G is the irradiance measured on the PV (W/m^2).

In a similar way, (Sahu *et al*., 2018) has proposed the same formula, but with:

$$T = Tamb + 1/U * \alpha * G * (1 - \eta) \tag{4}$$

And:

$$U = Uc + Uv * Velv \tag{5}$$

Where U is the thermal loss factor (W/m^2*ΔT), Uc is the thermal loss constant (W/m^{2}T), Uv is the wind proportional factor (W*s/m^3*ΔT) and $Velv$ is the local wind speed (m/s) and α is a fraction between the radiation

absorbed and the radiation reflected by the PV panel according to Lillo (2016).

An equation to predict the *DC PV* power is proposed (Mellit *et al*., 2020) in the literature. Considering a *PV* system with a size of *X* kW, the *DC* output power of this *PV* system at any given hour (h), can be expressed by the equation below:

$$PV(h) = \frac{X(h)*G}{1000} \; (6) \tag{6}$$

where, $PV(h)$ represents the *DC* output power of the *PV* system in kW at hour *h*, *G* denotes the solar irradiance in W/m^2 at hour *h* and 1000 is the solar constant in W/m^2.

Since certain data are lacking that may prevent the calculation of *T*, a mathematical approach to predict PV power as a function of irradiance and temperature measured on the module is proposed.

Indeed, it is noted that the *PV* power depends on *G* and *T*.

Since formula (3) only takes into account the ϕ factor depending on the temperature, we noted a difference of around 8% compared with the results of simulations of the model embedded in Matlab Simulink R2016a, which was chosen as the model for this study. Unfortunately, this equation incorporated into this software is not available on the interface, so it remains like a black box. In order to obtain results close to the simulation model, we added the term ω which is a variable coefficient taking into account the variation of *G* and *T* in order to adjust the efficiency according to variations in irradiance with respect to the reference value:

$$P_{thpv,p} = G * S * \eta * (1 + \phi * (T - Tref) + \omega) \tag{7}$$

$$with \; \omega = ((Gref - G)/Gref) * \phi * (T - Tref) \tag{8}$$

Then, this can be rewritten as:

$$P_{thpv,p} = G * S * \eta * (1 + \phi * (T - Tref) + \left(\frac{Gref-G}{Gref}\right) * \phi * (T - Tref)) \tag{9}$$

where, $P_{thpv, p}$ is the theoretical power of the solar panels (W) proposed, *G* the irradiance measured on the *PV* (W/m^2), $Gref$ is the reference irradiance (1000 W/m^2), *S* the surface area of the solar panels (m^2), η the PV efficiency, *T* the temperature measured on the panel (°C), Tref the reference temperature (25°C) and ϕ the temperature coefficient (/°C) (for UNISUN 150.2 modules, ϕ = -0.0043/°C and η = 0.165).

The energy produced is deduced by using the following formula (Lillo, 2016):

$$E_{thpv} = P_{thpv,s} \cdot t \tag{10}$$

18

where, $P_{thpv,s}$ is the simulated power (W) and t is the running time (h).

The *PR* performance ratio of the household is given by:

$$PR = \frac{E * G_{ref}}{P_{pv} * G(t)} \tag{11}$$

where, E is the daily energy (Wh), $G_{ref} = 1000$ W/m² and P_{pv} is the installed *PV* power.

Results and Discussion

To assess the objective of this study, simulations were carried out using Matlab Simulink R2016a for 10s, as the time taken for the results to converge is very long and requires a calculator as some studies limited their time (Kumar *et al.*, 2020). The variations in meteorological conditions over this time interval were then summarized. To assess the potential of the system (PV + storage) to secure the supply of local loads, PV power, Vdc voltage, power exchange and the state of charge and discharge of the batteries are the main parameters for assessing the system. Three representative scenarios are presented below:

o Interconnection of 2 autonomous households (having the same PV power but loads and irradiance different)
o Interconnection of 3 autonomous households with central storage (Households 1 and 2 are identical but Household 3 is different from them about load and irradiance)
o Interconnection of 3 autonomous households with central storage (Households 1 and 3 are identical in peak power but the peak power of Household 2 is double)

• Interconnection of 2 autonomous households (having the same PV power but loads and irradiance different**)**

In this scenario, household 1 and household 2 have the same peak power of 600 Wp, but they have different loads and different irradiance between 2 and 4 s.

The results in Figs. (11-12) show that Household 1, with a load of 500 W (Fig. 11c), does not draw its energy from its PVs or from the grid, but from its battery, which supplies 500W (Fig. 11b) from 0-0.5 s, because Ppv <506 W condition A of the energy management strategy is met: This is autonomous operation. Between 0.5 and 2 s, Ppv >506 W, the first household is connected to the second household. It is observed that its load is powered by its PVs and draws energy from household 2 to recharge its batteries (Figs. 11 and 12d) condition B of the energy management strategy is met. The latter is disconnected from the grid between 2 and 2.5 s because household 2 is disconnected according to its command (if Ppv <60W, no dispatching), so it becomes autonomous and in this

interval, Ppv <506 W: condition *C* of the energy management strategy is verified. This drop in PV power is due to the gradual increase in temperature from 25-45°C (Fig. 7), which reduces the *PV* voltage (Ngoma *et al.*, 2022; Juma *et al.*, 2021; Aït Cheikh *et al.*, 2007). After this period, the interconnection becomes permanent according to the household 1 control. From t = 8 s, Ppv <0 and household 1 is supplied by its battery and some of the energy is drawn from the grid: Condition *D* of the energy management strategy is satisfied.
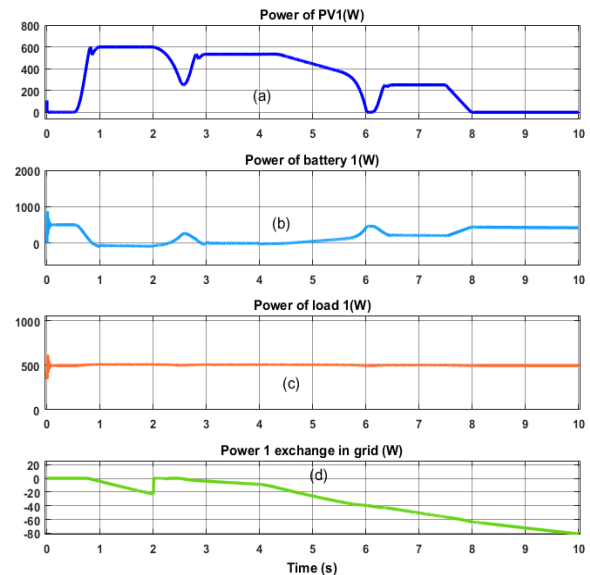

Fig. 11: Characteristics Power of household 1: a: PV power, b: Battery power, c: Load power (W) d: power 1 exchanged
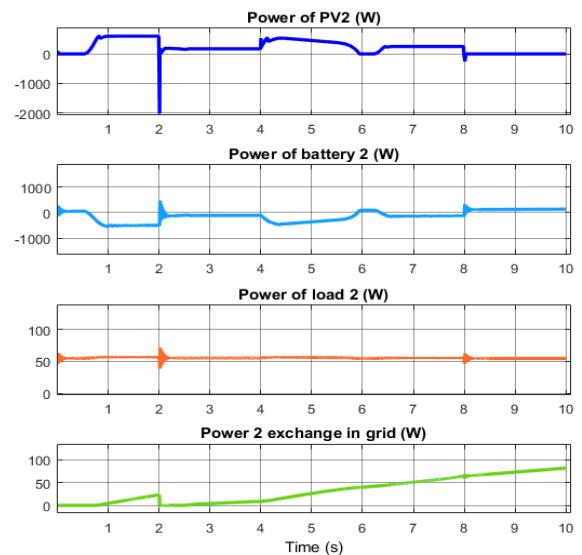

Fig. 12: Characteristics power of household 1: a: PV power, b: Battery power, c: Load power (W); d: Power 2 exchanged

The power curve of the PVs is the opposite of the power curve of the battery. This clearly shows that the battery receives its energy from the PVs. In fact, the battery recharges when its power decreases and discharges when its power increases.

Using the formula in the proposed Eq. (9), the predicted theoretical PV power $P_{thpv, p}$ between t = 6.5-7.5 s, where the average irradiance is 542 W/m² and the average PV temperature is 58°C (see the curves in Figs. 9-10) from data collected on 11 February 2022 for 7 h of sunshine (Ngoma *et al.*, 2022), is $P_{thpv, p}$ = 255.3 W, while the simulated value is 251.4 W. This is a difference of about 1.5% between the prediction formula and the simulation. If formula (3) is used, its power is 274.1W i.e. 8% of the difference.

Considering the formula (6) (Mellit *et al.*, 2020) which uses only the temperature of standard test conditions (25°C), under the irradiance of 542 W/m² and the temperature of the PVs at 25°C, the result is 325.2 W but with the proposed formula, it gave 321.9 W i.e., the difference about 1%. In the case of household 1, at t = 3 s, the predicted power $P_{thpv, p}$ is 542.9 W, compared with the simulated power (533.5 W) (Fig. 11a), a difference of around 1.73% is noted. On the other hand, using $P_{thpv, j}$ the result is 540.54 W, i.e. 1.3%.

For household 2 under shading between 2-4 s compared with household 1 (Fig. 9), the predicted power $P_{thpv, p}$ is 178.4 W and simulated 174 W, i.e. 2.1% of difference; with $P_{thpv, j}$ the result is 189.1 W, i.e., 8% difference. The predicted PV power results are close to those obtained from simulations. The maximum difference is about 2% with the proposed formula (9), whereas that of (Jie *et al.*, 2007), gave $P_{thpv,j}$ around 8%.

In this study, the robustness of the system by varying the load in the same household was not investigated, but only point loads in households were taken into account. On the other hand, an analysis of the system can be made to see the robustness of the system in load variation in the case of the Interconnection of 2 autonomous households (having the same PV power but different loads and irradiance) at the level of Figs. (11-12) in the interval of 6.5-7.5 s where the two households have the same weather conditions. Note that the greater the load, the greater the energy demand.

In fact, in this interval, a load of household 1 (500 W) is supplied by its PV, which produces 251 W and its battery which supplies around 216 W and draws an average of 45 W from household 2 (Fig. 11) meaning around 9% of efficiency thank to the interconnection. The result is close to that of Sayed *et al.* (2024).

With regard to the resilience of the system to changes in operating conditions, the robustness of the system after disconnection of the household from the grid between t = 2-2.5 s for household 1 is noted because the Ppv <0 and resumes its interconnection without ambiguity.

To assess the amount of energy produced by using formula (10), a PV productive energy of 1760 Wh for t = 7 h of sunshine on the day of 11 February for the household with 600 Wp is obtained (when the rate of G is 542 Wm² and T = 58°C); this corresponds to the performance ratio of 62% according to formula (11). The result is similar to that of Mellit *et al.* (2020). This energy produced can only supply the 1st household which has a load of 500 W during 3.5 h. Based on a household with a daily consumption of 1060 Wh, this household has an energy surplus of 700 Wh per day, i.e. 255 kWh/year. On the other hand, it can supply household 2 which has 50 W over a period of 35.8 h. With this energy for 24 h, household 2 gives a surplus of energy of around 592 Wh, enabling household 1 to operate for a further 1 h. This is verified by the power curves Figs. (11d and 12d) where household 2 transfers energy to household 1. This surplus was used to recharge electric vehicles in the work carried out by Salles-Mardones *et al.* (2022). The theoretical energy produced using the $P_{thpv, p}$ formula is 1787 Wh, i.e., 1.5% more than that simulated. The theoretical power prediction formula can be used to assess the energy performance of a PV array in an MG at a given time of day and the results of this approach are closer to the simulation values than those of Jie *et al.* (2007) and the formula goes beyond that of Mellit *et al.* (2020), which only stops at the reference temperature.

The new approach verified the literature affirmation which stipulates that, when the temperature increases, the PV power decreases Fig. (13); and when the irradiance increases, the PV power increases too, Fig. (14) (Ngoma *et al.*, 2022; Juma *et al.*, 2021; Aït Cheikh *et al.*, 2007).

In Fig. (13), the temperature is fixed and the irradiance is varied. Besides, Fig. (14) presented the fixed irradiance and the temperature variation.

The Table (6) resumes the comparative study between different methods.

With Ppv_s the simulation power, Ppv_j the power PV with Jie's method, Ppv_M the power PV with Mellit's method, and Ppv_p the Ppv power proposed.

Figures (15-16) show the characteristics of the PVs in households 1 and 2. The voltage of the PVs in household 2 drops until it reaches the negative values shown in Fig. (16) at 2 and 8 s; however, this drop does not occur in household 1. In fact, it is observed that the sudden variation in irradiance on the PVs leads to a sudden drop in voltage giving negative voltage values (Fig. 16a) at 2 and 8 where irradiance falls from 1000-350 W/m² and from 1000-542 W/m² respectively (Fig. 9), in contrast to household 1 where the drop in irradiance is not sudden (Fig. 8).

This drop occurs for 0.2 s and then returns to normal voltage (Fig. 17). Between 2 and 3 s, the PV powers decrease caused by the rise of the temperature of the panels.

Table 6: Comparison models

Description	Household1[6,5s-7,5s] :542W/m² ; 58°C		Household 1[3s] :1000 W/m² ; 45°C		Household 2[2s-4s] : 350 W/m² ; 45°C		Household1,2 : 542W/m² ; 25°C	
	Values	Différence	Values	Différence	Values	Différence	Values	Différence
Ppv_s (W)	251,4		533,5	---	174	---		
Ppv_j (W)	274,1	8%	540,5	1.3%	189.1	8%		
Ppv_M_(W)		-----	----	---			325,2	1%.
Ppv_p (W)	255,3	1.5%	542,9	1.73%	178.4	2.1%	321.9	
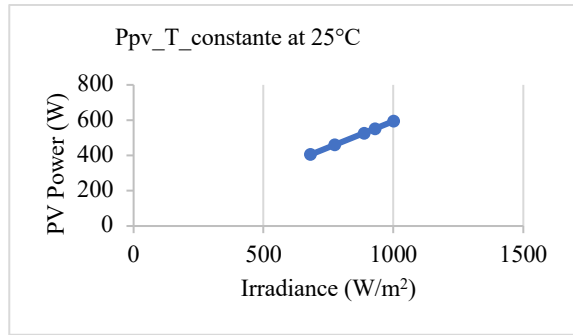
Fig. 13: Variation of PV power with irradiance when Temperature is constant
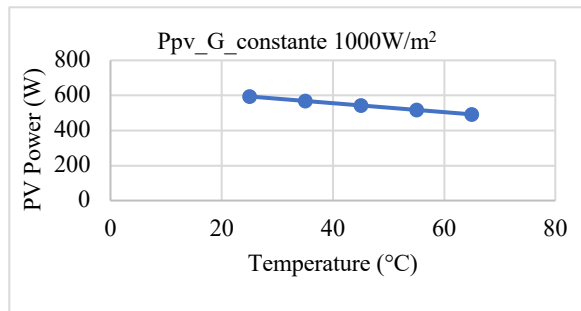
Fig. 14: Variation of PV power with Temperature when irradiance is constant

Fig. 15: Characteristics of PV1; a: PV1 Voltage (V); b: PV1 Current (A); c: PV1 power (W)
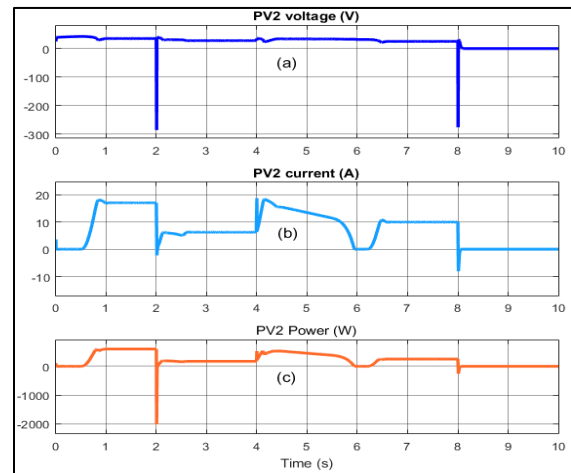
Fig. 16: Characteristics of PV2; a: PV2 Voltage (V); b: PV2 Current (A); c: PV2 power (W)
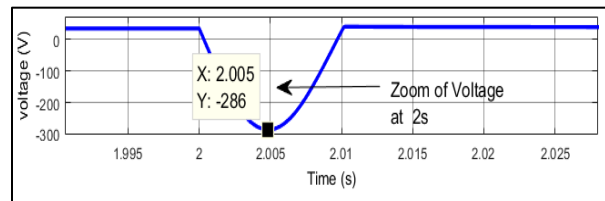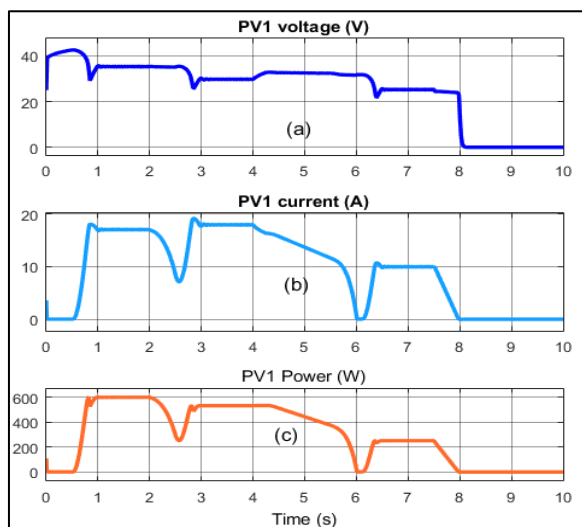

Fig. 17: PV voltage zoom at 2 s of PV2

In these curves, it is noted that PV power is linked to variations in meteorological conditions with irradiance variation predominating (Kewat *et al.*, 2018). This abrupt variation in irradiance has a temporary effect on the load of the household.

The behavior of the batteries in households 1 and 2 during interconnection is represented in Figs. (18-19). It is observed that the battery current in Fig. (19b) is the opposite of its voltage in Figs. (18a and 19a) respectively for each household. This demonstrates that when the voltage increases, the battery recharges by storing a current. These results are in agreement with (Harish *et al.*, 2019). The SOC curve in Fig. (18d) discharges more rapidly than in Fig. (19d) because the load on household 1 is 500 W. From 1-2 s, battery 1 recharges. After 8 s, the batteries in households 1 and 2 discharge more rapidly. It is shown that the battery of Household 2 has a large discharge gradient because it is now compensating for both loads. To reduce this rapid discharge, household 2 could disconnect from household 1 to work as a stand-alone system.

The Vdc (Fig. 20) is maintained at the set voltage, the maximum value of this being 52 V when the state of charge is 100% and 42 V when the battery is at 80%, grace to PI control. From 0-0.1 s, the voltage fluctuates because the two sources are paralleled and their voltages are not yet equal. These results are confirmed by Chaib *et al.* (2016) who stipulate that when two generators are associated in a system, the voltage of the DC bus takes time before stabilizing; this affects the whole system. It has been observed that voltage depends on changes in weather conditions as confirmed (Li and Ho, 2021).

After studying 2 households, in the following subsection, the interconnection of 3 households with central storage is conducted, in order to validate the reliability of the energy dispatching.
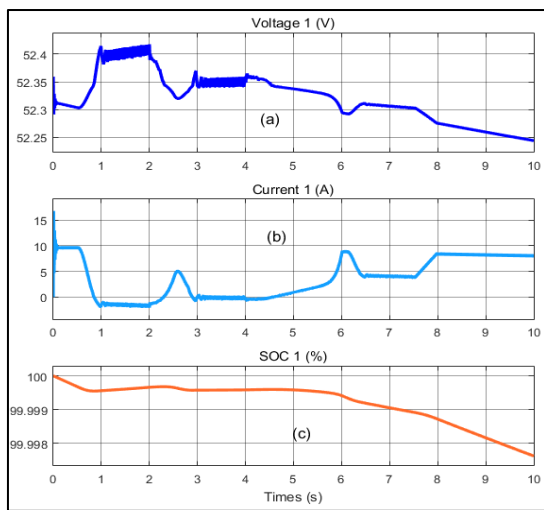
Fig. 18: State of the battery household 1; a: Voltage; b: current; c: State of charge
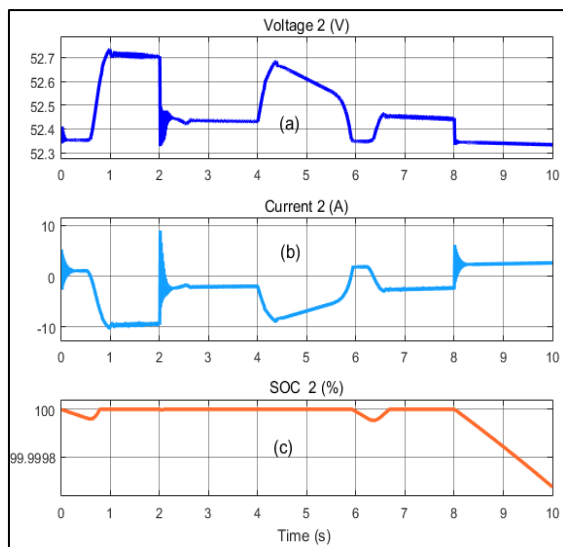

Fig. 19: State of the battery household 2; a: Voltage; b: current; c: State of charge
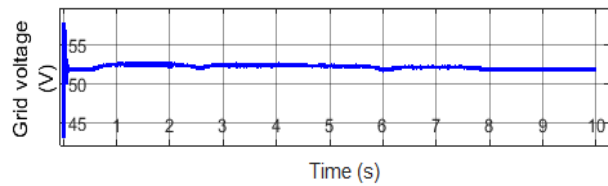

Fig. 20: Grid voltage

Interconnection of 3 Households with Central Storage

In this case with central storage, households 1 and 2 are identical in load (500 W) and meteorological conditions and household 3 has a load (50 W), and the irradiance different from them. Household 2 in the previous cases becomes household 3 due to its different irradiance.

The grid voltage (Fig. 21) is not stable until t = 0.3 s because of the household voltages, which are not equal as they all fluctuate. After that time, the voltage becomes stable and fluctuates for 0.1s at t = 0.9 s when the common load is connected and at t = 2 s and 2.29 s following disconnection of households 3, 1 and 2 respectively from the grid before reconnecting.

The Figs. (22-24a-c) do not change compared to the case of the Interconnection of households 1 and 2 with different loads and irradiance. It is observed only the change at the energy transfer level Figs. (22 and 24d). Household 1 has the same operation (PV generation and energy transfer or demand) as Household 2 because they are identical.

Households 1 and 2 can only send power to the grid when their PV power is greater than their load (506 W), otherwise, they draw power from the grid between 0-3 s for household 1 and between 0-2.5 s for household 2. After that time, the interconnection of these households is permanent. At t = 2.29 s, the power of PV1 and PV2 falls below the set power (506 W) for about 0.5 s as a result of the increase in the temperature of the PVs from 25-45°C; this cancels the power transfer in these households so that they reconnect from 2.86 s as shown in Figs. (22-23), at which time the power of PV1 and PV2 exceeds 506 W. In Fig. (24d), energy cancels out at t = 2 s because PV3 power becomes less than 60 W and reconnects after 0.1 s.

When the connection is permanent, households 1 and 2 only send surplus PV power to the grid up to t = 6.2 s and discharge their batteries after this time, this is similar to Sayed *et al.* (2024). However, household 3 only sends power to the grid when the peak power is greater than 60 W, i.e., greater than the load (50 W). The condition only applies from 0-3.5 s and then the interconnection becomes permanent. It has been noted that household 3 does not extract power from the grid but rather transfers it to the grid (Fig. 24d.) since its load (50 W) is lower than its PV power produced (Fig. 24c.) demonstrating the energy compensation. These results show the robustness of the proposed model and are similar to the model of Sayed *et al.* (2024); Hoffmann and Ansari (2019).
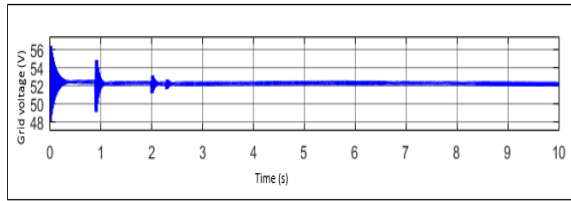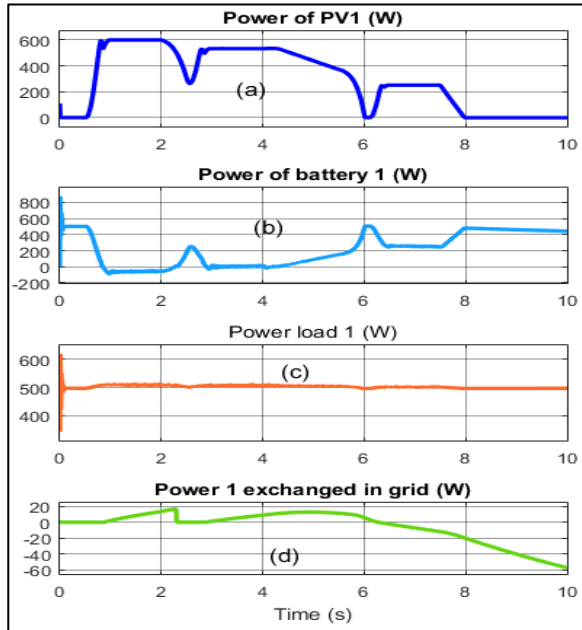
Fig. 21: Grid voltage

Fig. 22: Characteristics Power of household 1; a: PV power; b: Battery power; c: Load power (W); d: Power 1 exchanged
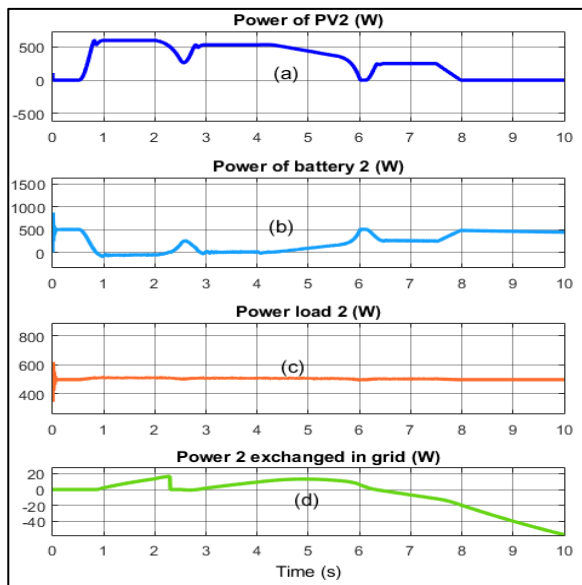

Fig. 23: Characteristics Power of household 2; a: PV power; b: Battery power; c: Load power (W); d: power 2 exchanged
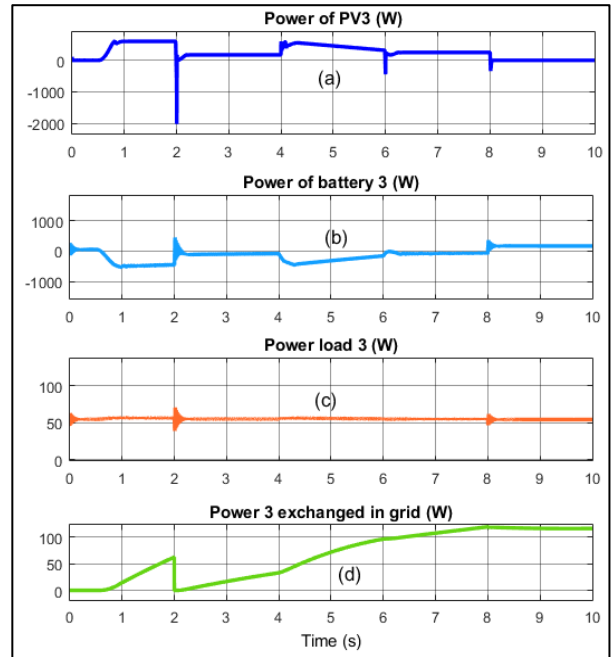

Fig. 24: Characteristics Power of household 3; a: PV power; b: Battery power; c: Load power (W); d: Power 3 exchanged

When the connection becomes permanent for all households, there is no longer any imbalance in the grid despite variations in meteorological conditions, which shows the reliability of this DC MG for interconnected autonomous PV households. These results corroborate those of Niti (2017); Eu-Tjin *et al.* (2016), which confirm the improvement in system reliability.

Figure (25) represents the state of charge of batteries in households 1, 2, 3 and central. The batteries of all households are discharging from 0-0.7 s because the PV power is lower than the set power load and they are recharged until t = 2.5 s. After t = 2.5 s, the batteries are discharged but proportionally to the irradiance.

The battery in household 3 (SOC^3) is fully charged after t = 0.7 s because the load power (50 W) is less than Ppv. With no PV power at t=8 s, battery 3 discharges rapidly because it is not only supplying its load but also compensating for the load of the other households, in this case, the common load (Fig. 26c).

Since battery C is common, it does not charge because the surplus of *PV* power is low, since it supplies the common load (200 W), Fig. (26c). This battery will charge when the common load is disconnected and the grid has a surplus.

After observation, it is recommended not to connect the common load when the interconnection of the households is not yet established, as this load delays the synchronization of the system.
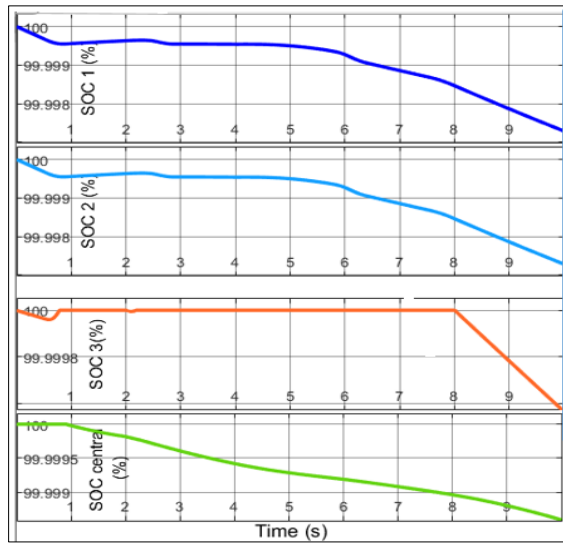
Fig. 25: State of batteries of three households interconnected with central battery with same peak power of 600 Wp
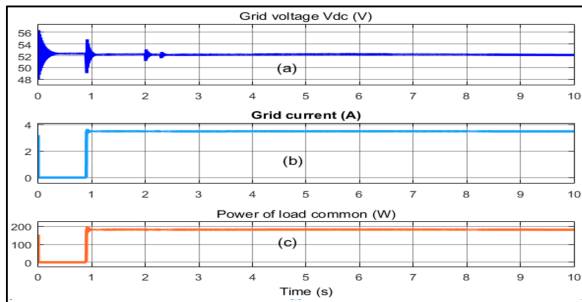

Fig. 26: Grid characteristic; a: Grid voltage; b: Grid current; c: Power of common load

Estimation of the Discharge Time

The discharging time for batteries of households 1 and 2 interconnected to the grid when the irradiance is at 542 W/m^2 between t = 6.2-7.5 s, the discharge rate is 0.00025%/s. This means 320,000 s (88.8 h) to reach 80% equivalent to 42 V, which is the limit voltage of the grid. When irradiance becomes zero at t = 8 s, PV = 0, the battery will take 112,000 s to discharge, i.e., 31.1 h for a power of 500 W.

Figure (27) represents the available power in the grid. The power available is the surplus from households in overproduction. This power increases as a function of irradiance and is drawn by households in deficit and the common load.

A study when the peak power of household 2 is doubled (1200 Wp) as presented below is also conducted.

It is noted that household 2 supplies more energy to the grid thanks to its high PV power, while the others have 600 Wp. The performance ratio of this household between 6.5 and 7.5 is still 62%. The result is similar to that of (Mellit *et al.*, 2020).

The simulated power in this interval is 502W, whereas the predicted power is $P_{thpv, p}$= 510.68 W, i.e., a difference of around 2%. Formula (2) gives $P_{thpv, j}$ = 548.27 W, i.e., a difference of 8% to that simulated.

Figure (28) represents the state of charge of the batteries of households 1, 2, 3, and central when household 2 has more peak power (1200 Wp) than the other two (600 Wp). The first household's battery (Fig. 28a) is discharging slowly due to its load (500 W). The battery in household 2 is at 100% from 1.5 s-5.9 s because its power PV2> Pcharge2, explaining the power transferred by this household is greater (Fig. 28d) than in the previous case where PV2 was 600 Wp (Fig. 25d).

Since battery C is common, it hardly charges at all (Fig. 28d) because of the low surplus of PV power in the grid (Fig. 29), since it supplies the common load (200 W). Comparing the power sent in the grid when household 2 has 1200 Wp to the previous case, the difference is around 47%. It is mentioned that the rate of discharge is slower than in the previous case when all households had the same peak power (600 Wp), thanks to the surplus in household 2. After t = 8 s, Ppv = 0 for all households, which increases the rate of battery discharge. These results are similar to those of Li and Ho (2021).

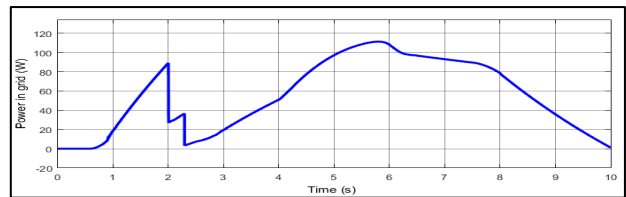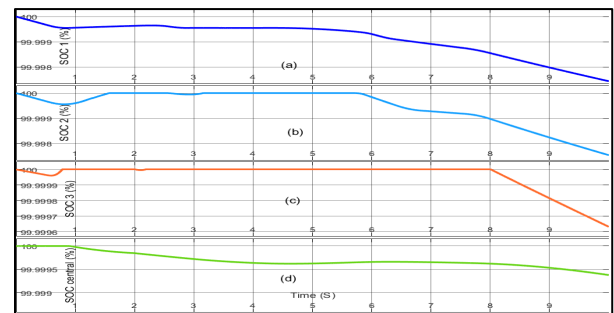**Fig. 27:** Power sent in the grid

Fig. 28: State of batteries of three households interconnected with central battery with different peak power
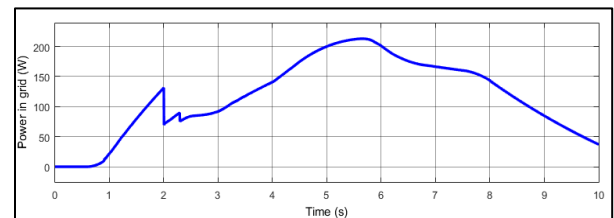

Fig. 29: Power sent in the grid when household 2 has 1200 Wp

24

Conclusion

This study has analyzed the operation of DC interconnected households under meteorological conditions. The interconnection of households improved the performance of the household that is under production by extracting power into the other household (grid) and adding its efficiency at around 9%. The study showed that weather conditions have an impact on energy production. As the management system is individual, the mathematical approach to power prediction has enabled prosumers to program their control switches according to the time of day or the power that their PV could produce using meteorological data. The proposed MG solution offers the advantage of individual management according to the photovoltaic power produced. In this model, it was shown that the operation of a household is not disrupted by the disconnection or reconnection of another household thanks to the voltage which is maintained at the consigned value, but on the other hand, the system showed that the common load is disrupted, although slightly when households are disconnected or reconnected to the network. It is therefore conceivable that, in future work, it would be interesting to:

1. Filter the bus voltage to avoid disturbances to the common load when the household disconnects or reconnects from the grid.
2. Implement the proposed formula in the simulation software
3. Count the energy exchanged between households by placing a meter
4. Evaluate the losses as a function of the distance between households in order to see how robust the system is over long distances
5. Interconnect several households in order to detect other factors that could influence the system
6. Carry out an experimental study

Acknowledgment

Funding Information

Author's Contributions

Gilbert Ngoma: Drafted the initial manuscript, contributed to methodology, conducted investigations, and participated in review and editing.

Maryse Dadina Nkoua Ngavouka: Provided resources, contributed to methodology and participated in written, review and edited.

Azeddine Houari: Developed software, provided resources, contributed to methodology and conducted investigations.

Léonide Messo, Resources: Provided resources and contributed to methodology and review.

Bernard M'Passi-Mabiala: Supervised the project.

Ethics

By signing below, we affirm that this study is solely the product of my own efforts. We have appropriately cited all sources of information and data utilized in my research and have clearly indicated their origins.

References

Ahshan, R., Iqbal, M. T., Mann, G. K. I., & Quaicoe, J. E. (2010). Micro-grid system based on renewable power generation units. *CCECE 2010*, 1–4. https://doi.org/10.1109/ccece.2010.5575112

Aït Cheikh, M. S., Larbes, C., Tchoketch Kebir, G. F., & Zerguerras, A. (2007). Maximum power point tracking using a fuzzy logic control scheme. *Journal of Renewable Energies*, *10*(3), 387. https://doi.org/10.54966/jreen.v10i3.771

Al-Ismail, F. S. (2021). DC Microgrid Planning, Operation and Control: A Comprehensive Review. *IEEE Access*, *9*, 36154–36172. https://doi.org/10.1109/access.2021.3062840

Central Electricity Authority (CEA). (2017). *Load Generation Balance Report 2017-18*. Central Electricity Authority (CEA).

Chaib, A., Achour, D., & Kesraoui, M. (2016). Control of a Solar PV/wind Hybrid Energy System. *Energy Procedia*, *95*, 89–97. https://doi.org/10.1016/j.egypro.2016.09.028

Choobineh, M., Arabnya, A., Khodaei, A., & Zheng, H. (2023). Game-theoretic peer-to-peer solar energy trading on blockchain-based transaction infrastructure. *E-Prime - Advances in Electrical Engineering, Electronics and Energy*, *5*, 100192. https://doi.org/10.1016/j.prime.2023.100192

El-Shahat, A., & Sumaiya, S. (2019). DC-Microgrid System Design, Control and Analysis. *Electronics*, *8*(2), 124. https://doi.org/10.3390/electronics8020124

Elsied, M., Oukaour, A., Gualous, H., & Lo Brutto, O. A. (2016). Optimal economic and environment operation of micro-grid power systems. *Energy Conversion and Management*, *122*, 182–194. https://doi.org/10.1016/j.enconman.2016.05.074

Eu-Tjin, C., Huat, C. K., & Seng, L. Y. (2016). Control strategies in energy storage system for standalone power systems. *4th IET Clean Energy and Technology Conference (CEAT 2016)*. 4th IET Clean Energy and Technology Conference (CEAT 2016), Kuala Lumpur, Malaysia. https://doi.org/10.1049/cp.2016.1268

Gil-González, W., Montoya, O. D., Grisales-Noreña, L. F., Cruz-Peragón, F., & Alcalá, G. (2020). Economic Dispatch of Renewable Generators and BESS in DC Microgrids Using Second-Order Cone Optimization. *Energies*, *13*(7), 1703. https://doi.org/10.3390/en13071703

Harish, V. S. K. V., Anwer, N., & Kumar, A. (2019). Development of a Peer to peer electricity exchange model in micro grids for rural electrification. *2019 2nd International Conference on Power Energy, Environment and Intelligent Control (PEEIC)*, 259–263. https://doi.org/10.1109/peeic47157.2019.8976848

Hoffmann, M. M., & Ansari, D. (2019). Simulating the potential of swarm grids for pre-electrified communities – A case study from Yemen. *Renewable and Sustainable Energy Reviews*, *108*, 289–302. https://doi.org/10.1016/j.rser.2019.03.042

Jie, J., Hua, Y., Gang, P., Bin, J., & Wei, H. (2007). Study of PV-Trombe wall assisted with DC fan. *Building and Environment*, *42*(10), 3529–3539. https://doi.org/10.1016/j.buildenv.2006.10.038

Juma, M., Mwinyiwiwa, B. M. M., Msigwa, C. J., & Mushi, A. T. (2021). Proposal Design of a Hybrid Solar PV-Wind-Battery Energy Storage for Standalone DC Microgrid Application. *Energies*, *14*, 5994. https://doi.org/10.20944/preprints202108.0264.v1

Kewat, S., Singh, B., & Hussain, I. (2018). Power management in PV-battery-hydro based standalone microgrid. *IET Renewable Power Generation*, *12*(4), 391–398. https://doi.org/10.1049/iet-rpg.2017.0566

Kong, K. G. H., Lee, A. G. J., Teng, S. Y., Leong, W. D., Orosz, Á., Friedler, F., Sunarso, J., & How, B. S. (2024). The P-graph application extension in multi-period P2P energy trading. *Renewable and Sustainable Energy Reviews*, *200*, 114544. https://doi.org/10.1016/j.rser.2024.114544

Kumar, J., Agarwal, A., & Singh, N. (2020). Design, operation and control of a vast DC microgrid for integration of renewable energy sources. *Renewable Energy Focus*, *34*, 17–36. https://doi.org/10.1016/j.ref.2020.05.001

Li, D., & Ho, C. N. M. (2021). A Module-Based Plug-n-Play DC Microgrid With Fully Decentralized Control for IEEE Empower a Billion Lives Competition. *IEEE Transactions on Power Electronics*, *36*(2), 1764–1776. https://doi.org/10.1109/tpel.2020.3009631

Lillo, P. (2016). *Manual and Evaluation of a Single-Phase Photovoltaic Array at the Residential Level in Chile. for the Sizing Bachelor's Thesis*. Federico Santa Maria Technical University.

Lonkar, M., & Ponnaluri, S. (2015). An overview of DC microgrid operation and control. *IREC2015 The 60th International Renewable Energy Congress*, 1–6. https://doi.org/10.1109/irec.2015.7110892

Lopes, J. A. P., Moreira, C. L., & Madureira, A. G. (2006). Defining Control Strategies for MicroGrids Islanded Operation. *IEEE Transactions on Power Systems*, *21*(2), 916–924. https://doi.org/10.1109/tpwrs.2006.873018

Madaci, B., Chenni, R., Kurt, E., & Hemsas, K. E. (2016). Design and control of a stand-alone hybrid power system. *International Journal of Hydrogen Energy*, *41*(29), 12485–12496. https://doi.org/10.1016/j.ijhydene.2016.01.117

Mellit, A., Massi Pavan, A., Ogliari, E., Leva, S., & Lughi, V. (2020). Advanced Methods for Photovoltaic Output Power Forecasting: A Review. *Applied Sciences*, *10*(2), 487. https://doi.org/10.3390/app10020487

Mwinyiwiwa, B. M. M. (2013). DC bus voltage regulator for renewable energy based microgrid application. *World Academy of Science, Engineering and Technology International Journal of Electrical, Robotics, Electronics and Communications Engineering*, *7*(12), 1139–1143.

Necaibia, A., Bouraiou, A., Ziane, A., Sahouane, N., Hassani, S., Mostefaoui, M., Dabou, R., & Mouhadjer, S. (2018). Analytical assessment of the outdoor performance and efficiency of grid-tied photovoltaic system under hot dry climate in the south of Algeria. *Energy Conversion and Management*, *171*, 778–786. https://doi.org/10.1016/j.enconman.2018.06.020

Nejat, C. (2022). Nejat Control Gain Series Method. *2022 IEEE 3rd Global Conference for Advancement in Technology (GCAT)*, 1–5. https://doi.org/10.1109/gcat55367.2022.9972147

Ngoma, G., Ngavouka, M. D. N., Mayala, T. S., Messo, L., & M'Passi-Mabiala, B. (2022). Study of the Performance of Mini PV Plant: Case Study of UNISUN 150.12M PV Module. *Applied Solar Energy*, *58*(4), 567–582. https://doi.org/10.3103/s0003701x22040089

Ngonda, T., Nkhoma, R., & Ngonda, V. (2023). Perceptions of Solar Photovoltaic System Adopters in Sub-Saharan Africa: A Case of Adopters in Ntchisi, Malawi. *Energies*, *16*(21), 7350. https://doi.org/10.3390/en16217350

Nikmehr, N., Najafi-Ravadanegh, S., & Khodaei, A. (2017). Probabilistic optimal scheduling of networked microgrids considering time-based demand response programs under uncertainty. *Applied Energy*, *198*, 267–279. https://doi.org/10.1016/j.apenergy.2017.04.071

Niti, A. (2017). Government of India. In *Draft National Energy Policy*.

Overen, O. K., & Meyer, E. L. (2022). Solar Energy Resources and Photovoltaic Power Potential of an Underutilised Region: A Case of Alice, South Africa. *Energies*, *15*(13), 4646. https://doi.org/10.3390/en15134646

Phurailatpam, C., Sangral, R., Rajpurohit, B. S., Singh, S. N., & Longatt, F. G. (2015). Design and analysis of a DC microgrid with centralized Battery Energy Storage System. *2015 Annual IEEE India Conference (INDICON)*, 1–6. https://doi.org/10.1109/indicon.2015.7443215

Querini, P. L., Chiotti, O., & Fernández, E. (2020). Cooperative energy management system for networked microgrids. *Sustainable Energy, Grids and Networks*, *23*, 100371. https://doi.org/10.1016/j.segan.2020.100371

Sahu, S., Panda, G., & Yadav, S. P. (2018). Dynamic Modelling and Control of PMSG based Stand-alone Wind Energy Conversion System. *2018 Recent Advances on Engineering, Technology and Computational Sciences (RAETCS)*, 1–6. https://doi.org/10.1109/raetcs.2018.8443850

Salles-Mardones, J., Flores-Maradiaga, A., & Ahmed, M. A. (2022). Feasibility Assessment of Photovoltaic Systems to Save Energy Consumption in Residential Houses with Electric Vehicles in Chile. *Sustainability*, *14*(9), 5377. https://doi.org/10.3390/su14095377

Sayed, M. A., Ahmed, M. M., Azlan, W., & Kin, L. W. (2024). Peer to peer solar energy sharing system for rural communities. *Cleaner Energy Systems*, *7*, 100102. https://doi.org/10.1016/j.cles.2023.100102

Schwarz, M. B., Mathilde, V., & Clausse, M. (2023). Impact of Flexibility Implementation on the Control of a Solar District Heating System. *Solar*, *4*(1), 1–14.

Seme, S., Sredenšek, K., Štumberger, B., & Hadžiselimović, M. (2019). Corrigendum to "Analysis of the performance of photovoltaic systems in Slovenia" [Sol. Energy 180 (2019) 550–558]. *Solar Energy*, *190*, 92. https://doi.org/10.1016/j.solener.2019.07.049

Sun, Q., Xing, D., Alafnan, H., Pei, X., Zhang, M., & Yuan, W. (2019). Design and test of a new two-stage control scheme for SMES-battery hybrid energy storage systems for microgrid applications. *Applied Energy*, *253*, 113529. https://doi.org/10.1016/j.apenergy.2019.113529

Tan, X., Li, Q., & Wang, H. (2013). Advances and trends of energy storage technology in Microgrid. *International Journal of Electrical Power & Energy Systems*, *44*(1), 179–191. https://doi.org/10.1016/j.ijepes.2012.07.015

Vadirajacharya, & Katti, P. K. (2012). Rural Electrification Through Solar and Wind Hybrid System: A Self Sustained Grid Free Electric Power Source. *Energy Procedia*, *14*, 2081–2087. https://doi.org/10.1016/j.egypro.2011.12.1211

Zaouche, F., Rekioua, D., Gaubert, J.-P., & Mokrani, Z. (2017). Supervision and control strategy for photovoltaic generators with battery storage. *International Journal of Hydrogen Energy*, *42*(30), 19536–19555. https://doi.org/10.1016/j.ijhydene.2017.06.107

Zhang, C., Wu, J., Zhou, Y., Cheng, M., & Long, C. (2018). Peer-to-Peer energy trading in a Microgrid. *Applied Energy*, *220*, 1–12. https://doi.org/10.1016/j.apenergy.2018.03.010